CMOS-COMPATIBLE MICROFABRICATION OF LAMINATED NIFE CORES FOR WIRELESS POWER TRANSFER

Xuan Wang, Sida Chen, Zihan Zhang, Lei Gu, and Mark G. Allen
University of Pennsylvania, USA

ABSTRACT

We present a CMOS-compatible microfabrication approach to laminated metallic magnetic cores for wireless power transfer (WPT) applications. An electrodeposited laminated NiFe core with a thickness of 1.5 mm is fabricated and tested as the receiver (RX) core in a 500 kHz magnetic coupling resonant wireless power transfer (MCR-WPT) system. The use of electrodeposition for the core preserves CMOS compatibility, while the formation of the core with laminations enables high frequency operation due to suppressed eddy current loss. The system achieves an output power of approximately 3 W across a 10 mm gap and a DC-DC efficiency of 50.1%. A non-CMOS-compatible commercial ferrite N97 core tested under identical conditions achieved a comparable 50.6% efficiency with a similar output power. This NiFe laminated material emerges as a compelling alternative to ferrite, providing comparable performance while offering the advantages of CMOS-compatibility and straightforward integration.

KEYWORDS

Wireless power transfer (WPT), magnetic coupling resonant wireless power transfer (MCR-WPT), sequential multilayer electrodeposition, laminated NiFe core, MEMS.

INTRODUCTION

Wireless power transfer (WPT) has experienced significant developments in recent years due to its untethered nature, making it a preferred technology utilized across various applications [1]. These applications span from low-power devices such as mobile phones [2] and biomedical implants [3] to high-power scenarios such as electric vehicles (EVs) [4] and aerospace equipment [5]. Among the various WPT methods, magnetic coupling resonant wireless power transfer (MCR-WPT) system has emerged as a highly popular method due to its excellent transmission efficiency and its ability to cover relatively long transmission distances [6], [7]. A key feature of MCR-WPT is its incorporation of a resonance compensation network to eliminate the reactive power component in the circuit, thereby achieving higher efficiency in active power transmission [7], [8]. Additionally, MCR-WPT systems often employ magnetic cores composed of permeable magnetic materials to enhance coupling performance and achieve magnetic concentration [9], [10].

Soft ferrite materials are the most widely used magnetic material in MCR-WPT systems at present due to their high relative permeability and low loss tangent [11], [12]. However, ferrite fabrication is not CMOS-compatible, making it challenging to contemplate a fully integrated WPT chip. Additionally, many ferrites are brittle, complicating their mass production [11] and use in applications requiring durability and robustness against mechanical shocks or harsh temperature variations. Moreover, there is a tradeoff in many ferrite cores between operating frequency and saturation flux density. Many higher frequency ferrites have a saturation flux density of approximately 500 mT [7], which could be a limiting factor for achieving high power density. In comparison, metallic alloys, such as permalloy, theoretically provide better power handling capacity due to their higher saturation flux density [13]. However, their considerably lower resistivity compared to ferrite can result in significant eddy current loss, especially at high (0.1-10 MHz) frequencies when the thickness of magnetic cores exceeds the skin depth of the material [14].

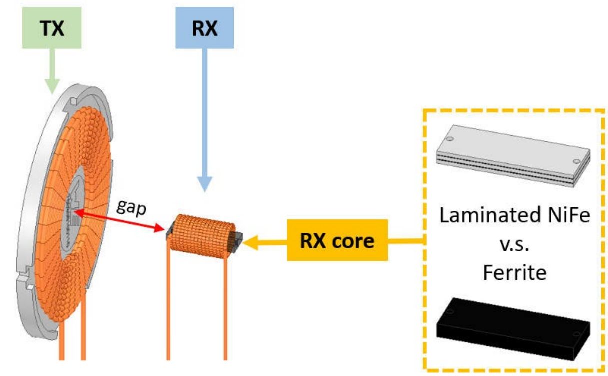

Figure 1: Schematic of the TX and RX coils in a magnetic resonance wireless power transfer system.

To address this issue, an alternating electroplating technique for metallic layers (NiFe) and insulation layers (polypyrrole) has been proposed to suppress eddy current loss [15], [16]. Optionally, the use of surface-tension-driven self-assembly [17] of stacked subcomponents enables the fabrication of a mm-scale thick core (although if desired, mm-scale plating molds could be employed instead) [18]. Unlike ferrites, which typically require high-temperature sintering, core electrodeposition through a photoresist mold not only offers flexibility in core geometry and thickness but is also inherently CMOS-compatible. This feature is particularly beneficial for applications requiring a miniaturized receiver (RX) coil, such as biomedical implantable devices. Moreover, varying the thickness of laminated metallic layers can effectively adjust the compatibility of the core with different frequencies. Thinner laminations can enable cores to operate at higher frequencies, thereby facilitating efficient power transfer at elevated frequency ranges.

In this paper, we focus on the fabrication and performance validation of such a laminated NiFe core within an MCR-WPT system, specifically as an RX core operating at 500 kHz. Additionally, we conduct a comparative analysis of the fabricated core efficacy against a commercial ferrite N97 core of the same size. The choice of the commercial ferrite N97 for comparison is due to its high permeability and moderate power loss, making it a suitable representative of MnZn ferrites widely utilized in wireless charging. This research aims to provide insights into the advantages and limitations of the proposed core design and its potential application in wireless power transfer systems.

EXPERIMENT OVERVIEW

Core Fabrication Process

The fabrication process of the laminated NiFe core is shown in Fig. 2. First, a seed layer of 200 nm Ti and 1 µm Cu was sputtered onto a 4-inch fused silica wafer, followed by the lithographic patterning of an electrically insulating photoresist mold (AZ4620,

978-1-940470-05-4/HH2024/$25©2024TRF
DOI 10.31438/TRF.HH2024.93

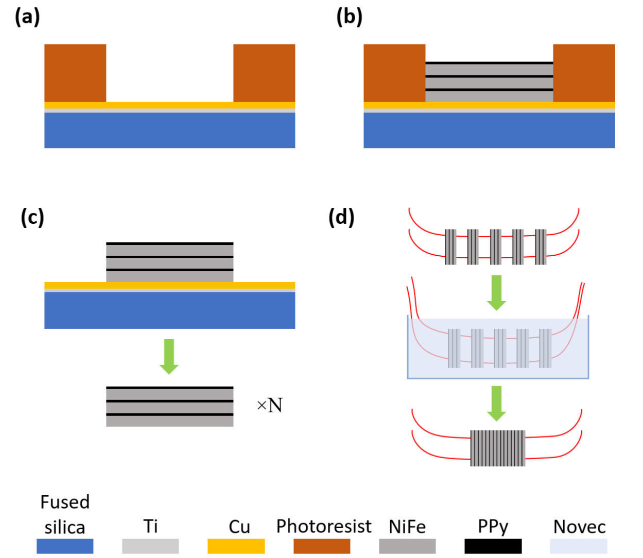

Figure 2: Fabrication process of the laminated NiFe core. (a) seed layer and mold preparation; (b) sequential electrodeposition; (c) mold removal and multilayer constructs release; (d) optional self-assembly.

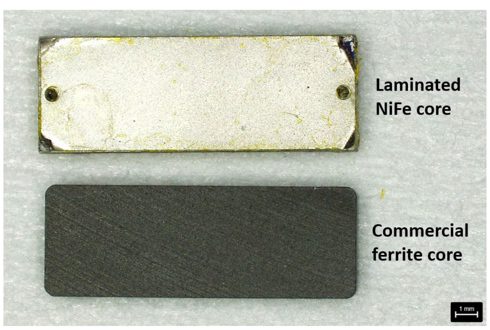

Figure 3: Photograph of the laminated NiFe core and a commercial ferrite N97 core.

MicroChem) to define the lateral extents of the multilayer cores [see Fig. 2(a)]. Subsequently, alternating sequential electrodeposition of NiFe and interlayer polypyrrole (PPy) was performed within the mold using an automated plating robot [see Fig. 2(b)]. The electrodeposition process utilizes a three-bath system, starting with the deposition of the NiFe layer, followed by the polypyrrole layer, and concluding with a thin Ni strike layer to activate the polymer surface for subsequent NiFe electrodeposition. An automated robot facilitates the transfer of the wafer between these three baths, repeating the electrodeposition cycle until the desired numbers and thicknesses of layers are achieved. Detailed electrodeposition procedures, including bath compositions and plating current densities, are provided in [15]. Afterwards, the photoresist mold was dissolved using acetone, and the NiFe/PPy multilayer constructs were detached from the wafer substrate by etching the Cu seed layer using a commercial copper etchant (Copper Etch BTP, Transene) [see Fig. 2(c)]. Finally, a self-assembly approach was exploited to transform the multilayer constructs into a thick core [see Fig. 2(d)]: two commercial magnetic wires held the multilayer constructs in place through guiding holes as they were immersed in Novec 2704 solution; the constructs were coated with fluoropolymer insulation

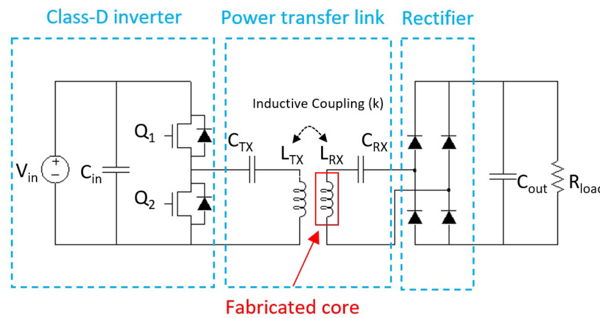

Figure 4: Schematic of the MCR-WPT system.

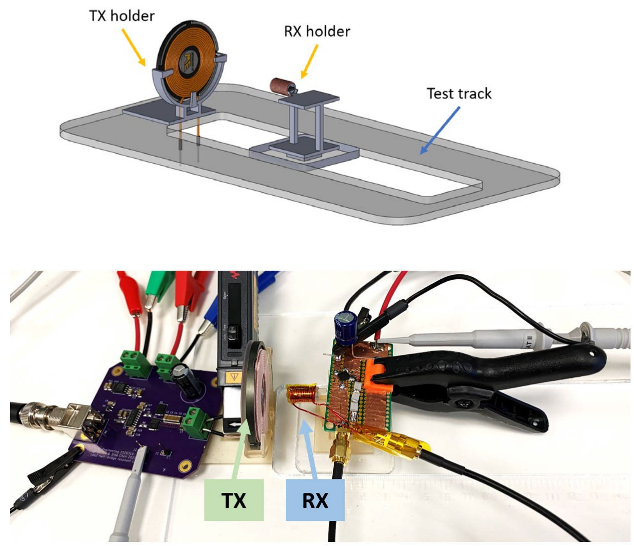

Figure 5: Experimental setup for MCR-WPT system, showcasing the model representation (top) and actual setup photograph (bottom).

and self-aligned upon solvent drying, forming a polymer-insulated assembly. More details regarding the surface tension-driven assembly can be found in [17].

To assess the efficacy of laminated NiFe as receiver cores compared to commercially available ferrite, the dimensions of the laminated NiFe were matched to those of the commercial ferrite bar, measuring 14 mm by 5 mm by 1.5 mm. Fig. 3 shows a side-by-side comparison of the laminated NiFe core and the commercial ferrite N97 core.

System Design

The fabricated laminated NiFe core and the commercial ferrite N97 core were tested as the RX core in an MCR-WPT system operating at 500 kHz. This system follows a series-series (SS) compensation topology [6], as depicted in Fig. 4. The power transmission process begins with a Class-D inverter implemented with a half-bridge circuit, which converts DC power into AC. The resulting AC power then enters the resonant tank, where the compensation capacitors C_{TX} and C_{RX} are carefully tuned to ensure resonance at the designed switching frequency of 500 kHz, thereby optimizing power transfer efficiency. The SS compensation network aims to achieve resonance, theoretically resulting in sinusoidal currents in both the TX and RX coils. On the RX side, the induced sinusoidal tank current is rectified by a full-bridge rectifier (CBRHDSH1-40L TR13 PBFREE, Central Semiconductor Corp). Additionally, a large output capacitor is placed in parallel with the DC load to smooth out ripples and maintain a stable DC output.

Within the wireless link setup, a commercial coil (760308100110, Würth Elektronik) was affixed to a 3D-printed TX holder and served as the TX coil. An adjustable RX holder, positioned on a laser-cut acrylic board with scales, facilitated precise adjustments in the TX-to-RX airgap for controlled testing. The core under test, either the ferrite N97 or the laminated electrodeposited core, was placed within the RX holder, around which 15 turns of magnetic wires were wound, functioning as the RX coil to capture the induced power from the TX coil. Fig. 5 provides a visual representation of the experimental setup, showcasing both the model and a photograph.

RESULTS AND DISCUSSION

The focus was on evaluating the output power and the DC-DC efficiency η_{DC} across varying airgaps ranging from 0mm to 20mm in increments of 5mm. The DC-DC efficiency is commonly expressed using the equations:

$$\eta_{DC} = \frac{P_o}{P_{in}} \quad (1)$$

$$P_{in} = V_{in} I_{in} \quad (2)$$

$$P_o = V_o I_o \quad (3)$$

where V_{in} and I_{in} represent the input voltage and current of the DC power supply, while V_o and I_o denote the output voltage and current to the DC load. Additionally, P_{in} and P_{out} refer to the input power from the power supply and output power to the DC load, respectively. Experiments were conducted with an input voltage set at 10 V, and a DC load resistance of 11 Ω is utilized.

Fig. 6 presents a comparison of the output power and DC-DC efficiency for the laminated NiFe and ferrite N97 cores across varying airgap distances. The experimental results reveal that both the NiFe and N97 cores exhibit a consistent decrease in efficiency as the airgap distance increases from 0 mm to 20 mm, as expected due to increased reluctance and leakage flux with larger airgaps. Both the NiFe and N97 cores exhibit peak output power at a 10 mm airgap distance. At larger distances, the output power falls off as expected. Since the compensation capacitors were not adjusted during the measurement, the fall-off of power at shorter distances could be attributed to the larger coupling factor affecting the resonance tuning of the primary and secondary circuits.

Notably, the laminated NiFe core demonstrates comparable performance to the ferrite N97 core across the range of airgap distances tested. They both reach their peak output power at the 10 mm airgap distance. At this critical point, the system utilizing the laminated NiFe core delivers 2.98 W with an efficiency of 50.1% to the load, at a DC output voltage of 5.79 V and a current of 0.52 A. In comparison, the system utilizing the ferrite N97 core achieves 3.24 W with a slightly higher efficiency of 50.6% to the load, at a DC output voltage of 6.03 V and a current of 0.54 A. The slightly higher efficiency for the ferrite core suggests that NiFe may have higher losses, possibly due to factors such as eddy current and hysteresis losses.

To address these losses and further improve the performance of NiFe cores, several strategies can be employed. For instance, to suppress eddy current losses, thinner laminations of NiFe (in this work the lamination thickness is 3 µm) can be electroplated, reducing the thickness through which eddy currents can circulate and thus decreasing the associated losses. Additionally, to mitigate

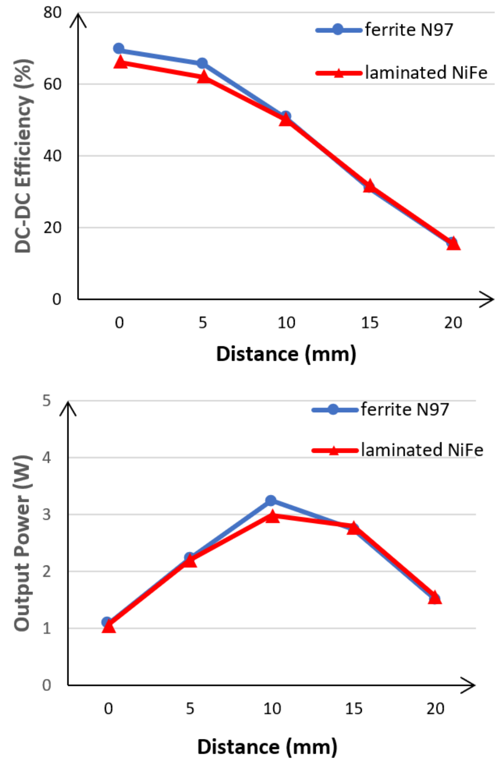

Figure 6: DC-DC efficiency and output power at load of the ferrite N97 core and laminated NiFe core for distance from 0 mm to 20 mm. The switching frequency was set to 500 kHz, matching resonant frequencies of both TX and RX side.

hysteresis losses, in-plane anisotropy can be induced in the NiFe material. This can be achieved by applying an additional magnetic field during the electroplating process [19], [20], [21], aligning the magnetic domains in a preferred direction and reducing the energy required to magnetize the material, thereby cutting down hysteresis losses.

These approaches highlight the potential for optimizing NiFe cores to achieve even higher efficiencies and performance levels, making them even more competitive and appealing for WPT applications. Besides, a system-level optimization of the WPT circuits, for example, selecting appropriate transmission frequencies and switching devices, can also significantly improve the system performance and better utilize NiFe cores.

CONCLUSION

A CMOS-compatible microfabrication method was employed to fabricate a laminated NiFe core using sequential multilayer electrodeposition. This laminated NiFe core was then evaluated as the RX core in an MCR-WPT system operating at 500 kHz. The laminated NiFe core demonstrates comparable performance to the commercial ferrite N97 core, delivering approximately 3 W with a 10 mm gap and achieving an efficiency of 50.1%. Such laminated NiFe cores, developed through CMOS-compatible microfabrication, emerge as a promising alternative to traditional ferrite cores for miniaturized systems.

ACKNOWLEDGEMENTS

This work was carried out in part at the Singh Center for Nanotechnology, which is supported by the NSF National Nanotechnology Coordinated Infrastructure Program under grant NNCI-2025608. The authors would like to thank Dr. Yixiao Ding at the University of Pennsylvania for his invaluable assistance and expertise during the 3D printing process.

REFERENCES

[1] Z. Zhang, H. Pang, A. Georgiadis, and C. Cecati, "Wireless Power Transfer—An Overview", *IEEE Transactions on Industrial Electronics*, 66, 1044 (2019).

[2] Y. J. Park, "Next-Generation Wireless Charging Systems for Mobile Devices", *Energies*, 15, 3119 (2022).

[3] S. R. Khan, S. K. Pavuluri, G. Cummins, and M. P. Desmulliez, "Wireless Power Transfer Techniques for Implantable Medical Devices: A Review", *Sensors*, 20, 3487 (2020).

[4] A. A. S. Mohamed, A. A. Shaier, H. Metwally, and S. I. Selem, "An Overview of Dynamic Inductive Charging for Electric Vehicles", *Energies*, 15, 5613 (2022).

[5] K. Song, B. Ma, G. Yang, J. Jiang, R. Wei, H. Zhang, and C. Zhu, "A Rotation-Lightweight Wireless Power Transfer System for Solar Wing Driving", *IEEE Transactions on Power Electronics*, 34, 8816 (2019).

[6] M. Abou Houran, X. Yang, and W. Chen, "Magnetically Coupled Resonance WPT: Review of Compensation Topologies, Resonator Structures with Misalignment, and EMI Diagnostics", *Electronics*, 7, 296 (2018).

[7] D. Wang, J. Zhang, S. Cui, Z. Bie, K. Song, C. Zhu, and M. I. Matveevich, "Modern Advances in Magnetic Materials of Wireless Power Transfer Systems: A Review and New Perspectives", *Nanomaterials*, 12, 3662 (2022).

[8] A. Kurs, A. Karalis, R. Moffatt, J. D. Joannopoulos, P. Fisher, and M. Soljačić, "Wireless Power Transfer via Strongly Coupled Magnetic Resonances", *Science*, 317, 83 (2007).

[9] C. Kim, D.-H. Seo, J.-S. You, J.-H. Park, and B.-H. Cho, "Design of A Contactless Battery Charger for Cellular Phone", 15th Annual IEEE Applied Power Electronics Conference and Exposition (APEC), New Orleans, LA, USA (2000), pp. 769 - 773.

[10] R. Bosshard, J. Mühlethaler, J. W. Kolar, and I. Stevanović, "Optimized Magnetic Design for Inductive Power Transfer Coils", 28th Annual IEEE Applied Power Electronics Conference and Exposition (APEC), Long Beach, CA, USA (2013), pp. 1812-1819.

[11] W. Peng and Z. Chen, "Enhanced Planar Wireless Power Transfer Systems with Ferrite Material", IEEE Wireless Power Transfer Conference (WPTC), Montreal, QC, Canada (2018), pp. 1-4.

[12] W. Ding and X. Wang, "Magnetically Coupled Resonant Using Mn-Zn Ferrite for Wireless Power Transfer", 15th International Conference on Electronic Packaging Technology, Chengdu, China (2014), pp. 1561-1564.

[13] C. R. Sullivan, B. A. Reese, A. L. F. Stein, and P. A. Kyaw, "On Size and Magnetics: Why Small Efficient Power Inductors Are Rare", International Symposium on 3D Power Electronics Integration and Manufacturing (3D-PEIM), Raleigh, NC, USA (2016), pp. 1-23.

[14] D. Flynn, A. Toon, L. Allen, R. Dhariwal, and M. P. Y. Desmulliez, "Characterization of Core Materials for Microscale Magnetic Components Operating in the Megahertz Frequency Range", *IEEE Transactions on Magnetics*, 43, 3171 (2007).

[15] M. Synodis, J. B. Pyo, M. Kim, H. Oh, X. Wang, and M. G. Allen, "Fully Additive Fabrication of Electrically Anisotropic Multilayer Materials Based on Sequential Electrodeposition", *Journal of Microelectromechanical Systems*, 29, 1510 (2020).

[16] J. B. Pyo, X. Wang, M. Kim, H. Oh, R. Kauffman, and M. G. Allen, "Suppression of Eddy Current Loss in Multilayer NiFe-Polypyrrole Magnetic Cores Fabricated Using a Continuous Electrodeposition Process", *Journal of Emerging and Selected Topics in Power Electronics*, 10, 7433 (2022).

[17] J. Kim, M. Kim, and M. G. Allen, "Surface Tension-Driven Assembly of Metallic Nanosheets at The Liquid-Air Interface: Application to Highly Laminated Magnetic Cores", 18th International Conference on Solid-State Sensors, Actuators and Microsystems (TRANSDUCERS), Anchorage, AK, USA (2015), pp. 2224-2227.

[18] J. Kim, "UV-LED Lithography for Millimeter-Tall High-Aspect Ratio 3d Structures", 20th International Conference on Solid-State Sensors, Actuators and Microsystems & Eurosensors XXXIII (TRANSDUCERS & EUROSENSORS XXXIII), Berlin, Germany (2019), pp. 100-103.

[19] J. Y. Park, S. H. Han, and M. G. Allen, "Batch-Fabricated Microinductors with Electroplated Magnetically Anisotropic and Laminated Alloy Cores", *IEEE Transactions on Magnetics*, 35, 4291 (1999).

[20] J. Kim, M. Kim, J. K. Kim, and M. G. Allen, "Anisotropic Nanolaminated CoNiFe Cores Integrated into Microinductors for High-Frequency DC-DC Power Conversion", *Journal of Physics D: Applied Physics*, 48 (2015).

[21] L. Yang, L. Gao, C. Chen, and Z. Liu, "Electrodeposition of Anisotropic NiFe Thin Films for Integrated High-Frequency Micro-Inductor", 19th International Conference on Electronic Packaging Technology (ICEPT), Shanghai, China (2018), pp. 1241-1245.

CONTACT

*X. Wang, tel: +1-215-316-4115; wxuan@seas.upenn.edu